# Axial and Radial Investigation of Hydrodynamics in a Bubble Column; Influence of Fluids Flow Rates and Sparger Type

Hélène Chaumat, Anne-Marie Billet, Henri Delmas

INTERNATIONAL JOURNAL OF CHEMICAL REACTOR ENGINEERING

*Volume* 4 2006 *Article* A25

# Axial and Radial Investigation of Hydrodynamics in a Bubble Column; Influence of Fluids Flow Rates and Sparger Type

Hélène Chaumat* Anne-Marie Billet†

Henri Delmas‡

*Laboratoire de Génie Chimique, Toulouse, Helene.Chaumat@ensiacet.fr

†Laboratoire de Génie Chimique, Toulouse, AnneMarie.Billet@ensiacet.fr

‡Laboratoire de Génie Chimique, Toulouse, Henri.Delmas@ensiacet.fr

ISSN 1542-6580

# Axial and Radial Investigation of Hydrodynamics in a Bubble Column; Influence of Fluids Flow Rates and Sparger Type

Hélène Chaumat, Anne-Marie Billet, and Henri Delmas

## Abstract

A detailed investigation of local hydrodynamics in a pilot plant bubble column has been performed using various techniques, exploring both axial and radial variations of the gas hold-up, bubble average diameter and frequency, surface area. A wide range of operating conditions has been explored up to large gas and liquid flow rates, with two sparger types. Two main complementary techniques were used: a quasi local measurement of gas hold-up via series of differential pressure sensors to get the axial variation and a double optic probe giving radial variations of gad hold-up, bubble average size and frequency and surface area.

According to axial evolutions, three zones, where radial evolutions have been detailed, have been separated: at the bottom the gas injection zone, the large central region or column bulk and the disengagement zone at the column top. It was found that significant axial and radial variations of the two phase flow characteristics do exist even in the so called homogeneous regime. The normalized profiles of bubble frequency appear sparger and gas velocity independent contrary to bubble diameter, gas hold-up and interfacial area normalized profiles. In any case bubbles are larger in the sparger zone than elsewhere.

The main result of this work is the very strong effect of liquid flow on bubble column hydrodynamics at low gas flow rate. First the flow regime map observed in batch mode is dramatically modified with a drastic reduction of the homogeneous regime region, up to a complete heterogeneous regime in the working conditions (uG$>$ 0.02 m/s). On the contrary, liquid flow has limited effects at very high gas flow rates.

A large data bank is provided to be used for example in detailed comparison with

CFD calculations.

**KEYWORDS:** bubble column, hydrodynamics, gas hold-up, bubble diameter, surface area, optic probe

# I. INTRODUCTION

Among industrial gas-liquid reactors, bubble columns are widely used and investigated. However, most studies on those reactors are restricted to global data, including global gas hold-up, volumetric mass transfer coefficient and the classical identification of hydrodynamics regimes.

Indeed, in bubble columns, three hydrodynamics regimes can be observed; each of them having a specific bubble size distribution.

_ In the homogeneous regime, the flow is governed by the primary bubbles formed at the sparger: nearly no radial nor axial evolution is observed and the bubble size distribution is rather narrow. This flow is observed at small superficial gas velocity.

_ At higher gas flow-rates, the heterogeneous regime is observed: the primary bubble predominance vanishes and the coalescence and break-up balance prevails. In this flow, the bubble size distribution is very wide. The large rising bubbles tend to migrate towards the column core while, near the wall, the small bubbles are on the whole descending. In this regime, large 3D vortices are observed but statistically, on very long observation times, the liquid follows large loops.

_ The change from homogeneous to heterogeneous regime is often progressive. The superficial gas velocity range corresponding to this change is called the transition regime.

This global knowledge on flow regimes should be completed with local information to identify zones of high mass transfer for instance. Such data is also essential for CFD validation which should not be ascertained only with global data. Considering the large experimental investigation needed to completely describe the gas and liquid local behavior, we focus this study on gas phase, and we supply key information concerning local gas hold-up, bubble size and interfacial area. The local description proposed here consists in estimating the radial and axial evolution of gas phase characteristics.

The bubble column is classically divided into three axial areas: the sparger area, the bulk area and the disengagement area. As previously mentioned, the relation between sparger and bulk areas depends on the hydrodynamics regime, that is to say on the gas velocity, on the media and on the column geometry. Those parameters condition the bubble formation (bubble size and distribution), the axial evolution of flow (bubble migration towards the column axis, symmetry, coalescence, break-up…), as well as the minimum height to reach the equilibrium (height above which there is no axial evolution). In the literature, time-averaged local profiles are often obtained near this equilibrium level. Note that this equilibrium is not easy to describe, as time-averaged gas hold-up profiles obtained by Yao et al. (1991) in the heterogeneous regime do not stabilize and become continuously more parabolic when going away from the sparger, even if the mean gas hold-up at each section remains constant.

_ Among time-averaged gas phase local data, gas hold-up is the easiest to measure and consequently, the most studied. Gas hold-up profiles often present a radial symmetry (Dziallas et al., 2000; Chen et al., 2001, for $D_C$=0.2m; Degaleesan et al., 2001, for $H_C$>0.5 m; Kemoun et al., 2001). However, some dissymmetry is sometimes observed; it can be due to:

- Sparger dissymmetry
- Liquid loop: the gas hold-up profiles obtained by Chen et al. (2001) is symmetric for $D_C$=0.2 m but some 3D effects appear when $D_C$=0.4 m.
- Slight deviation from vertical column
- Too short time investigations

The gas hold-up profiles are generally rather uniform at moderate gas flow-rates (Yao et al., 1991; Groën et al., 1995; Magaud et al., 2001). At higher gas flow-rates, they become bell-shaped with a maximum value on the axis (Yao et al., 1991; Groën et al., 1995). Such profiles are often characterized with a power law (Joshi and Sharma, 1979; Clark and Flemmer, 1987; Luo and Svendsen, 1991; Fischer et al., 1994; Groën et al., 1995; Kemoun et al., 2001). Note that, at low gas flow-rates, when a small diameter column is run with alcoholic additives, saddle or W-shaped profiles can be observed (Clark and Flemmer, 1987; Parasu Veera et al., 2001).

_ The bubble velocity profiles have the same gas flow-rate dependence as the gas hold-up profiles: uniform at low gas flow-rates, the profiles become parabolic when the gas flow-rate increases. Nevertheless, the parabolic shape appears at lower gas flow-rates: parabolic bubble velocity profiles are already observed in the homogeneous regime (Yao et al., 1991; Magaud et al., 2001). At high gas hold-up, the velocity profiles do not evolve with gas flow-rate: the liquid loop is stable.

_ Due to metrology limitations, few bubble size profiles are obtained in bubble column; only mean or axial values are usually measured.

In fact, most local data is gas hold-up data obtained in a restricted column part: little data concerns bubble size and still less its evolution along the column. Besides, local data is usually limited to low gas flow-rates and to

batch liquid flow. Although a liquid feed is widely used industrially, its effect is often neglected or limited to low superficial liquid velocities (around 0.01 m/s). Four studies at larger liquid velocity are reported in the literature (Zheng et al., 1988; Magaud et al., 2001; Moustiri et al., 2001; and Yang and Fan, 2003): they demonstrate that the liquid circulation induces a slight gas hold-up decrease and an increase in bubble velocity, mixing rate and turbulence. Nevertheless, this superficial liquid velocity effect seems linked up with the range of gas velocity (Alvarez Cuenca and Nerenberg, 1981).

The objective of this work is to describe the global (liquid and gas) and local (gas) hydrodynamics in a given apparatus in a large range of operating conditions. To complete the current data, the studied conditions sweep from classically described conditions (batch liquid flow, restricted gas flow rate, small hole sparger) to industrial conditions (liquid flow, high gas flow-rate, large hole sparger). In this way, a wide range of superficial gas and liquid velocity is studied and two perforated toric spargers are tested. The liquid used here is water to be compared to literature. This study constitutes a reference for a further investigation with organic liquid.

## 2. EXPERIMENTAL SET-UP

### 2.1. Experimental conditions

Experiments are performed in a pilot plant composed by a stainless steel bubble column reactor ($D_C$=0.2 m; $H_C$=1.6 m aerated liquid) completed with an external gas-liquid separator in order to achieve the recycling of liquid only (fig. 1). The liquid is circulated by a pump. Two spargers having 0.8% open area are used; each of them is composed of two toric rings of 0.10 and 0.15 m in diameter. Each sparger is pierced with a specific hole size: the first sparger has industrial type orifices ($d_0$=0.001 m), and the second one has thinner orifices ($d_0$=0.0005 m).

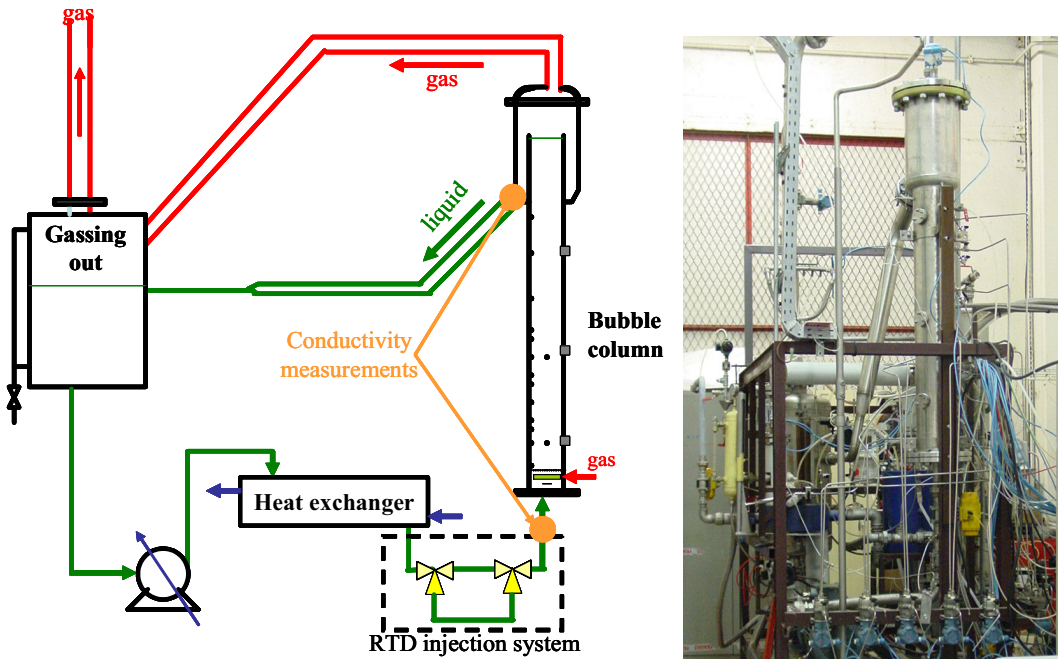


Figure 1. Experimental set-up

The liquid phase is tap water and the gas phase is air. Large ranges of superficial gas velocity (up to 0.30 m/s) and superficial liquid velocity (up to 0.12 m/s) have been investigated; they lead to global gas hold-up up to 35%. All experiments are run at atmospheric pressure and at 20°C; the temperature is controlled.

## 2.2. Measurement methods

This study requires several metrologies to investigate global and local hydrodynamics.

### 2.2.1. Global measurements

To describe the axial evolution of gas hold-up in the column, seven differential 'smart' pressure transducers (Rosemount, model 3051, fig. 2c), called DPi, are located as mentioned on figure 2a. As shown by Chaumat et al. (2005b), each DPi transducer leads to reliable estimation of the mean gas hold-up ($\varepsilon_{G,i}$) within the column part i. The DP7 transducer includes the whole column except the disengagement zone; it allows the calculation of the global gas hold-up, $\overline{\varepsilon}_G$, as well as the flow regime identification. DP1 to DP6 transducers are located on different 0.2 m high column sections in order to obtain the axial evolution of mean gas hold-up ($\varepsilon_G(DPi)=\varepsilon_{G,i}$). As specified in Chaumat et al. (in press), they can also be used to validate some local gas hold-up measurements.

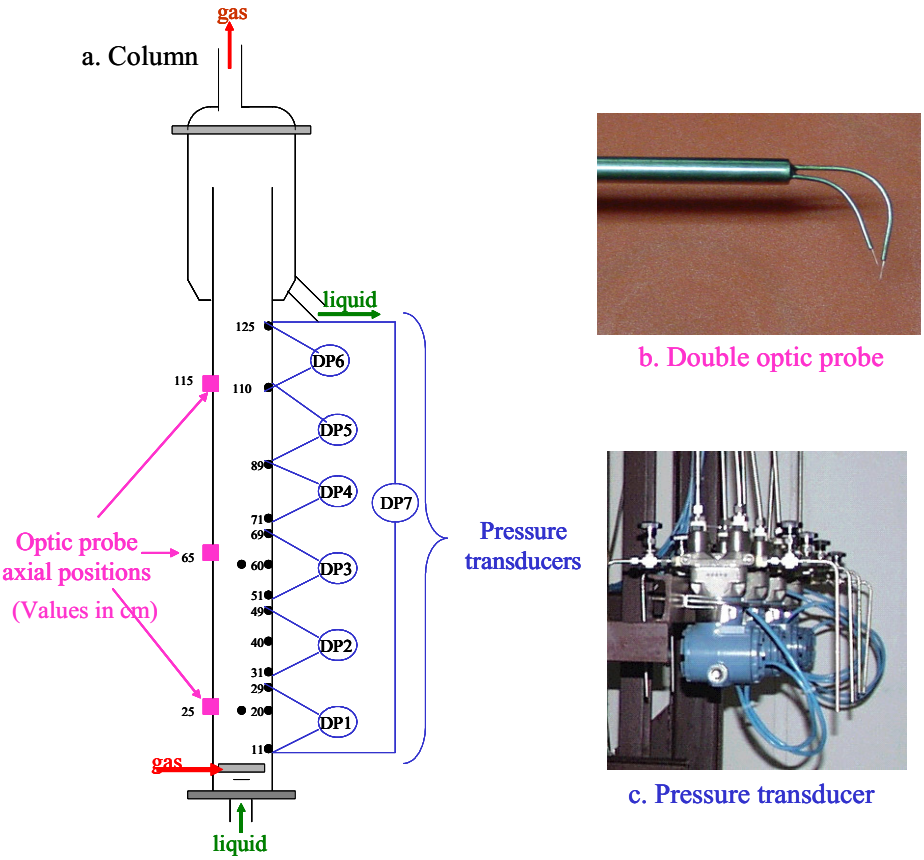


Figure 2. Hydrodynamic measurements: tools and positions

Experimental Residence Time Distributions (RTD) are obtained by tracer analysis (when liquid is fed): after a KOH pulse injection at the column bottom (about 10 g), the conductivity is recorded at the column inlet and outlet (cf. fig. 1a). Once the mean residence time ($\tau$) and the RTD variance ($\sigma^2$) are derived from input and output data, a number of equivalent perfectly mixed reactors (CSTR), $N_{CSTR}= \tau^2 / \sigma^2$, is associated to each experimental condition.

Note that some mass transfer measurements have also been performed in this apparatus; they are presented elsewhere (Chaumat et al, 2005a).

### 2.2.2. Local measurements

The gas phase is characterized at local scale using a commercial double optic probe (RBI), as it is the only metrology applicable in our conditions (opaque apparatus, hold-up higher than 10%), which is compatible with further use in organic media.

Each double optic probe is made of two 40 µm glass fibres whose tips are reinforced by two sharp sapphire sensing tips (fig. 2b). A small distance between probe tips ($l_{12}$) is chosen (0.0017 m in this work) to increase the proportion of bubbles pierced by both tips, leading to significant measurements. The data acquisition and treatment used are described elsewhere by Chaumat et al. (in press). This technique leads to time-averaged data of local gas hold-up, bubble frequency, interfacial area and mean Sauter diameter.

The double probe is set up inside a thin stainless steel bended support, so that it always faces the main vertical flow. Once settled, it can be moved along the column diameter, in order to investigate gas phase radial profiles.

Three axial positions have been selected (fig. 2a) in order to observe the flow near the sparger (h=0.25 m) and in the column bulk (h=0.65 and 1.15 m) and to analyze the axial evolution. The targeted heights have been deduced from a preliminary local study showing that the equilibrium is reached at around 0.5 m.

## 3. LIQUID BATCH CONDITIONS

Before the liquid flow effect is analyzed, the bubble column hydrodynamics is described in batch condition.

### 3.1. Global gas hold-up

Among other data, figure 3 presents the global gas hold-up ($\bar{\varepsilon}_G$) evolution versus the superficial gas velocity, for both spargers. We recall that the global gas hold-up is delivered by DP7.

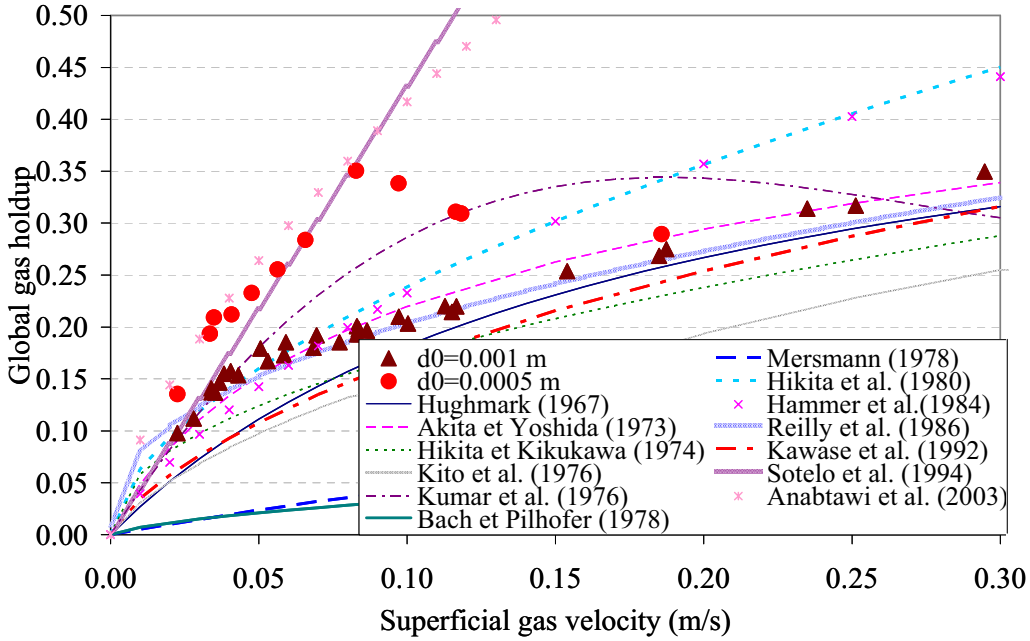


Figure 3. Global gas hold-up evolution versus superficial gas velocity. Comparison with previous correlations

Using classical methods described elsewhere (Chaumat et al., 2005b), this data leads to the hydrodynamics regimes identification presented in figure 4.

Very different behaviors are observed when changing the gas sparger:
- The homogeneous regime is maintained in a wide gas velocity range with the small hole sparger ($d_0$=0.0005m).
- The small hole sparger leads to higher gas hold-up in the low and intermediate gas velocity, corresponding to homogeneous and transitions regimes, than the large hole sparger.

Nevertheless, when the hydrodynamics regime is heterogeneous for both spargers, i.e. at high gas flow-rate ($u_G$>0.16 m/s), the gas hold-up does not depend any more on the gas sparger: the bubble distribution in the bulk is determined by the coalescence-break-up balance.

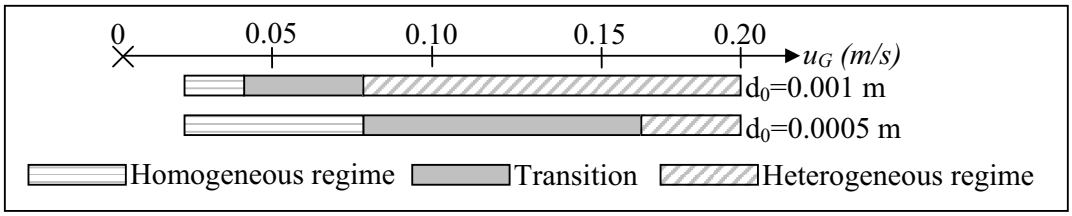


Figure 4. Hydrodynamic regime identification in batch conditions

Even if those behaviors are quite classical, the obtained gas hold-up curves do not compare well with the well-known empirical gas hold-up correlations (fig. 3). Figure 3 exhibits a large discrepancy between the 13 tested correlations (table 1). The main reason for this discrepancy is probably linked to the use of different gas spargers, as sparger characteristics are not accounted for in the correlations. Consequently, in the heterogeneous regime, when the gas sparger effect disappears, the agreement between the correlations improves and more correlations become consistent with our results. However, in this regime, major differences still persist between authors: the gas sparger is not the only overlooked or under-estimated parameter.

For the large hole gas sparger ($d_0$=0.001 m), the best agreement is found with Akita and Yoshida (1973) and Reilly et al. (1986) correlations. The former was established in similar conditions (perforated sparger, $u_G \leq 0.4$ m/s, $u_L \leq 0.044$ m/s, $D_C$=0.152-0.60 m, $H_C$=1.26-3.5 m) with a large set of experimental data. For the small hole gas sparger ($d_0$=0.0005 m), no convenient correlation is found for the whole gas flow-rate range, but Hughmark (1965) and Kawase et al. (1992) are satisfactory for the heterogeneous regime.

As a conclusion, the global correlations are not fully suitable for gas hold-up prediction, probably because they do not take into account some crucial parameters, such as sparger or column geometric characteristics or water quality.

### 3.2. Axial evolutions

The axial evolution of mean gas hold-up, issued from pressure transducers DP1 to DP6, is studied for each sparger. For a better readability, figure 5 presents, for each column part i, the relative difference between the mean gas hold-up and the global gas hold-up: $\varepsilon_{R,i} = \dfrac{\varepsilon_{G,i} - \overline{\varepsilon}_G}{\overline{\varepsilon}_G}$, for i=1 to 6 (remind that i=1 corresponds to the lowest location, see fig. 2).

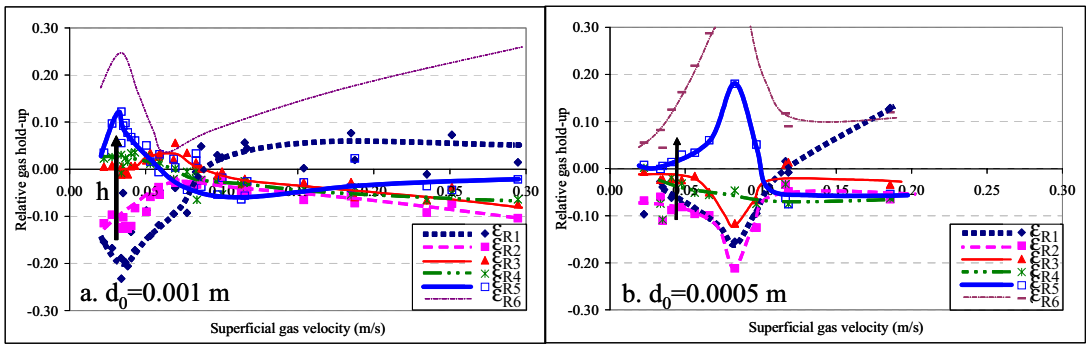


Figure 5. Axial evolution of the relative gas hold-up obtained for each sparger

Table 1. Gas hold-up correlations from literature

| Correlations | Authors |
|---|---|
| $\varepsilon_G = \dfrac{1}{[2+(\frac{0,35}{u_G})(\frac{\rho_L \sigma}{72})^{1/3}]}$ | Hughmark (1967)* |
| $\dfrac{\varepsilon_G}{(1-\varepsilon_G)^4} = C*(\dfrac{gD_C^2\rho_L}{\mu_L})^{1/8}(\dfrac{gD_C^3\rho_L^2}{\mu_L^2})^{1/12}(\dfrac{u_G}{\sqrt{gD_C}})$<br>C=0,2 for pure and non electrolytic liquids<br>C=0,25 for electrolytic liquids | Akita and Yoshida (1973)* |
| $\varepsilon_G = 0,505 u_G^{0,47}(\dfrac{0,072}{\sigma})^{2/3}(\dfrac{0,001}{\mu_L})^{0,05}$ | Hikita and Kikukawa (1974)* |
| $\varepsilon_G = 0,728U - 0,485U^2 + 0,0975U^3$<br>with: $U = u_G[\rho_L^2/(\sigma(\rho_L-\rho_G)g)]^{1/4}$ | Kumar et al. (1976)* |
| $\dfrac{\varepsilon_G}{[\varepsilon_G(1-\varepsilon_G)^2]^{0,44}} = 0,5\left(\dfrac{D_C u_G^2 \rho_L}{\sigma}\right)^{0,11}\left(\dfrac{u_G}{\sqrt{gD_C}}\right)^{0,22}$ | Kito et al. (1976)* |
| $\dfrac{\varepsilon_G}{(1-\varepsilon_G)} = 0,0115\left[\dfrac{u_G^3\rho_L^2}{\mu_L g(\rho_L-\rho_G)}\right]^{0,23}$ | Bach and Pilhofer (1978)* |
| $\dfrac{\varepsilon_G}{(1-\varepsilon_G)^4} = 0,14 u_G[\dfrac{\rho_L^2}{\sigma(\rho_L-\rho_G)g}]^{1/4}[\dfrac{\rho_L^2\sigma^3}{\mu_L^4(\rho_L-\rho_G)g}]^{1/24}(\dfrac{\rho_L}{\rho_G})^{5/72}(\dfrac{\rho_L}{\rho_L-\rho_G})^{1/3}$ | Mersmann (1978)* |
| $\varepsilon_G = 0,672 f(\dfrac{u_G\mu_L}{\sigma})^{0,578}(\dfrac{\mu_L^4 g}{\rho_L\sigma^3})^{-0.131}(\dfrac{\rho_G}{\rho_L})^{0,062}(\dfrac{u_G}{u_L})^{0,107}$<br>f=1,0 for non electrolytics liquids<br>f=$10^{0,04141}$ for I<1,0 kg ion/m$^3$<br>f=1,1 for I>1,0 kg ion/m$^3$<br>I : Ionic strengh | Hikita et al. (1980)* |
| $\dfrac{\varepsilon_G}{1-\varepsilon_G} = 0,4 u_G^{0,87}\rho_L^{0,1}\rho_G^{0,17}\sigma^{-0,06}\mu_L^{-0,21}g^{-0,27}$ | Hammer et al. (1984) |
| $\varepsilon_G = 296 u_G^{0,44}\rho_L^{-0,98}\rho_G^{0,19}\sigma^{-0,16} + 0,009$ | Reilly et al. (1986) |
| $\dfrac{\varepsilon_G}{1-\varepsilon_G} = 0,0625\left(\dfrac{u_G^3\rho_L}{\mu_L g}\right)^{1/4}$ | Kawase et al. (1992) |
| $\varepsilon_G = 129(\dfrac{u_G\mu_L}{\sigma})^{0,99}(\dfrac{\mu_L^4 g}{\sigma_L\sigma^3})^{-0,123}(\dfrac{\rho_G}{\rho_L})^{0,187}(\dfrac{\mu_G}{\mu_L})^{0,343}(\dfrac{d_p}{D_C})^{-0,089}$ | Sotelo et al. (1994) |
| $\varepsilon_G = 0,66 u_G^{0,66}\mu_L^{-0,24}H^{-0,38}\sigma^{0,22}\rho_L^{0,02}$ | Anabtawi et al. (2003) |

* cf. Shah et al. (1982)
(all dimensional quantities are in S.I. units)

Figure 5 shows that the amplitude of the relative difference to the mean gas hold-up is rather complex but similar for both spargers (less than 20% for $\varepsilon_{G,1}$ to $\varepsilon_{G,5}$). Significant changes of axial profiles are observed when changing flow regimes by varying gas velocity (see also fig. 6): at low gas velocity, therefore

homogeneous regime, $\varepsilon_G$ is continuously increasing from the sparger to the column top. Note that only a very short homogeneous regime part is 'ideal', that is to say with no axial and radial evolution. Such a trend is observed only with the small hole sparger at the lowest gas velocity (fig. 6b, $u_G$=0.035 m/s). This observation is confirmed by local measurements with the optic probe: no clear axial evolution is observed in gas hold-up and bubble frequency with the small hole sparger for $u_G$=0.035 m/s (fig. 7). However, in these conditions, some axial discrepancies are already found on bubble size and interfacial area as the bubbles are greater in the sparger area than above (as shown on fig. 7). At higher gas velocity (cf. fig. 6a, $u_G$=0.066 m/s) and/or larger hole sparger (cf. fig. 6b, $u_G$=0.066 m/s and fig. 8, $u_G$=0.037 m/s), no data homogeneity is yet observable. The classical homogeneous regime description appears then oversimplified.

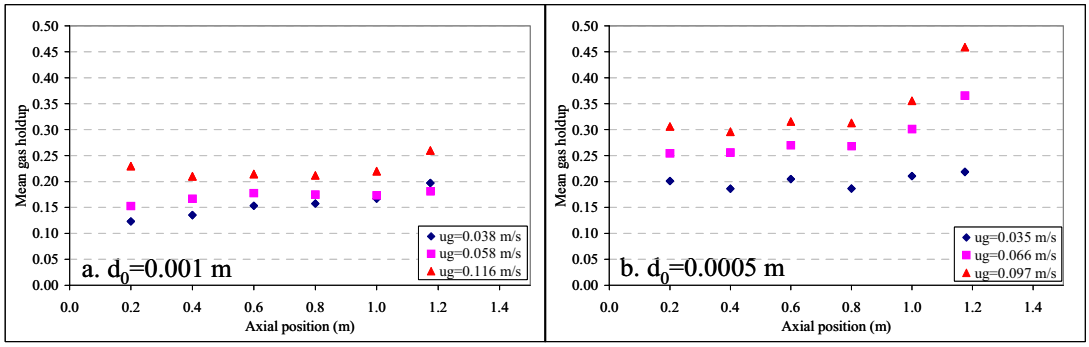


Figure 6. Axial evolution of the mean gas hold-up for each sparger

The gas hold-up axial gradient reaches a clear maximum (fig. 5) at about 0.03 m/s and 0.08 m/s with the large and small hole sparger respectively, velocity corresponding to the homogeneous regime end (fig. 4). After this peak in relative gas hold-up, the mean gas hold-up increases axially too (fig. 6a, $u_G$=0.058 m/s or fig. 6b, $u_G$=0.097 m/s), but this tendency is reduced when superficial gas velocity increases until it disappears in the heterogeneous regime. For local data, see as an example the case $u_G$=0.118 m/s on figure 7 ($d_0$=0.0005 m).

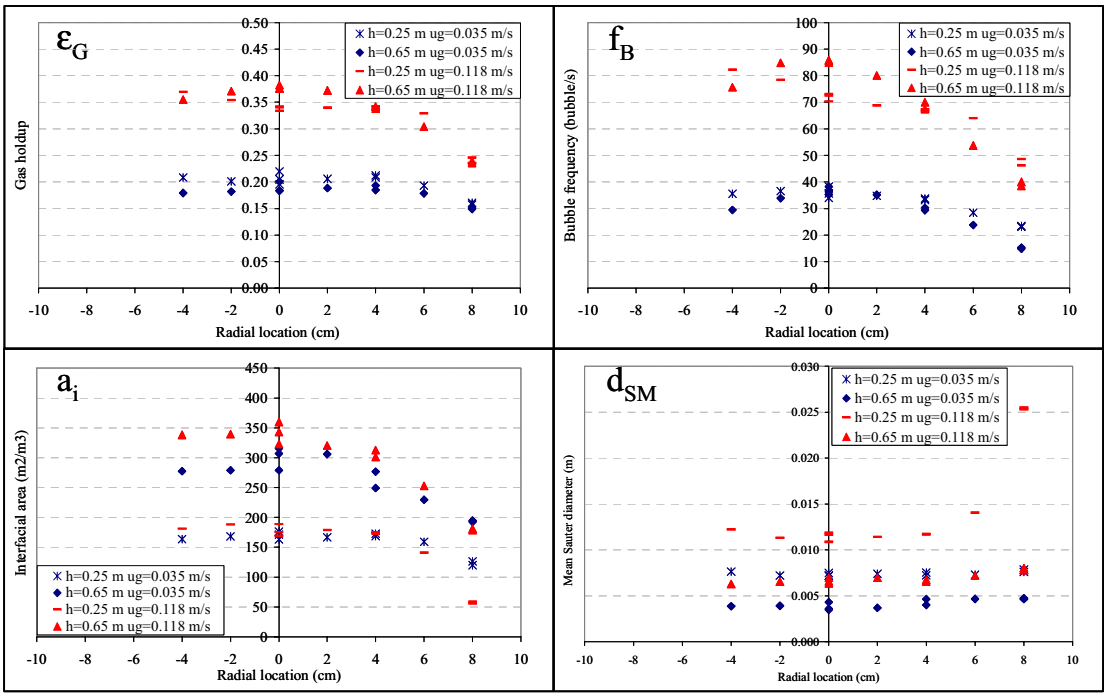


Figure 7. Axial evolution of profiles obtained with the small hole sparger ($d_0$=0.0005 m)

At high gas velocity - i.e. heterogeneous regime - gas excess is found both in the sparger and disengagement zones, whereas in the bulk, the gas hold-up axial evolution is weak (fig.6a, $u_G$=0.116 m/s). Those behaviors are also observable on local data ($u_G$=0.117 on fig. 8):

- The bubble frequency and the interfacial area are weaker at the bottom, because of higher bubble diameter: large bubbles are formed and tend to break-up during their rise to reach equilibrium.

- As for the bulk flow, neither global nor local data present significant difference between the two levels h=0.65 m and h=1.15 m (fig. 7 and 8). The intermediate level h=0.65 m has been selected for further investigations as some measurements with the small hole sparger at 1.15 m height stands in the disengagement area (that is why this level is not presented on figure 7). Note that it induces that the disengagement area is sparger dependent and can have significant height, particularly in a moderately high column.
Figure 5 also reveals the respective extension of the three zones (sparger, bulk and disengagement). Their respective heights depend on operating conditions: the sparger area ends between 0.3 and 0.5 m (i.e. $H_C/D_C$=1.5-2.5) and the disengagement area begins above 1.10 m (i.e. $H_C/D_C \geq 5.5$). Note that, in the heterogeneous regime, the sparger area is small: the coalescence-break-up balance is quickly obtained.

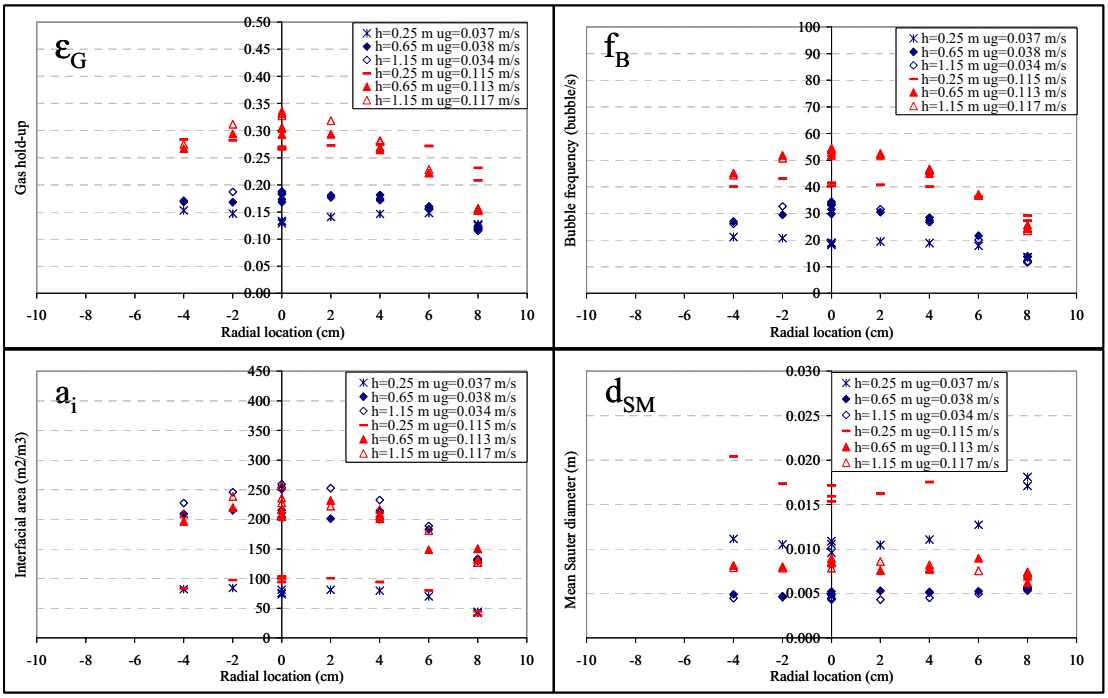


Figure 8. Axial evolution of profiles obtained with the large hole sparger ($d_0$=0.001 m)

To go deeper into the local observations, the column bottom (h=0.25 m) and the column bulk (h=0.65 m) are analyzed in details in the following.

## 3.3. Column bottom analysis (h=0.25 m)

Figure 9 shows the local profiles of time-averaged gas hold-up, bubble frequency, interfacial area and mean Sauter diameter observed at column bottom for each sparger and for three superficial gas velocities. The gas hold-up, bubble frequency and interfacial area profiles are rather bell-shaped, while the mean Sauter diameter profiles are bowl-shaped.

### 3.3.1. Sparger effect

Due to the sparger geometry (toric rings of 0.10 and 0.15 m in diameter), the bubbles are not formed near the column axis. As a consequence, we observe at the bottom large bubbles (issued from jets) on the side and small bubbles on the axis, contrary to classical bulk profiles. As bubbles tend to migrate to the axis (the bubble frequency is greater on the axis), such an injection leads to quite flat gas hold-up profiles, but not to homogeneous gas distributions. Gas distribution is clearly uniform at $u_G$=0,037 m/s with the small hole sparger only, when the 'ideal' homogeneous regime is observed.

On the other hand, the small hole sparger forms smaller bubbles leading to higher gas hold-up, higher interfacial area and particularly higher bubble frequency values compared with the large hole sparger. The bubble frequency and gas hold-up profile shapes also depend on the sparger: at high gas velocity, they are not symmetrical yet when using the small hole sparger, whereas, in any other case, all profiles seem satisfactorily symmetrical.

### 3.3.2. Gas velocity effect

Whatever the gas sparger, when the superficial gas velocity increases from 0.035 m/s to 0.083 m/s, the gas hold-up, bubble frequency and bubble size values clearly rise, while for further gas flow-rate increase, those values evolve slightly. It could be related to the bubble injection regime: the jet regime is observed from around 0.04 m/s for the large hole sparger and around 0.08 m/s for the small hole sparger (i.e. for $Re_0 \approx 1000$, Heijnen and Van't Riet, 1984). At a superficial gas velocity of 0.035 m/s, the jet regime is not reached for any of the two spargers; at 0.083 m/s, it is reached in both cases.

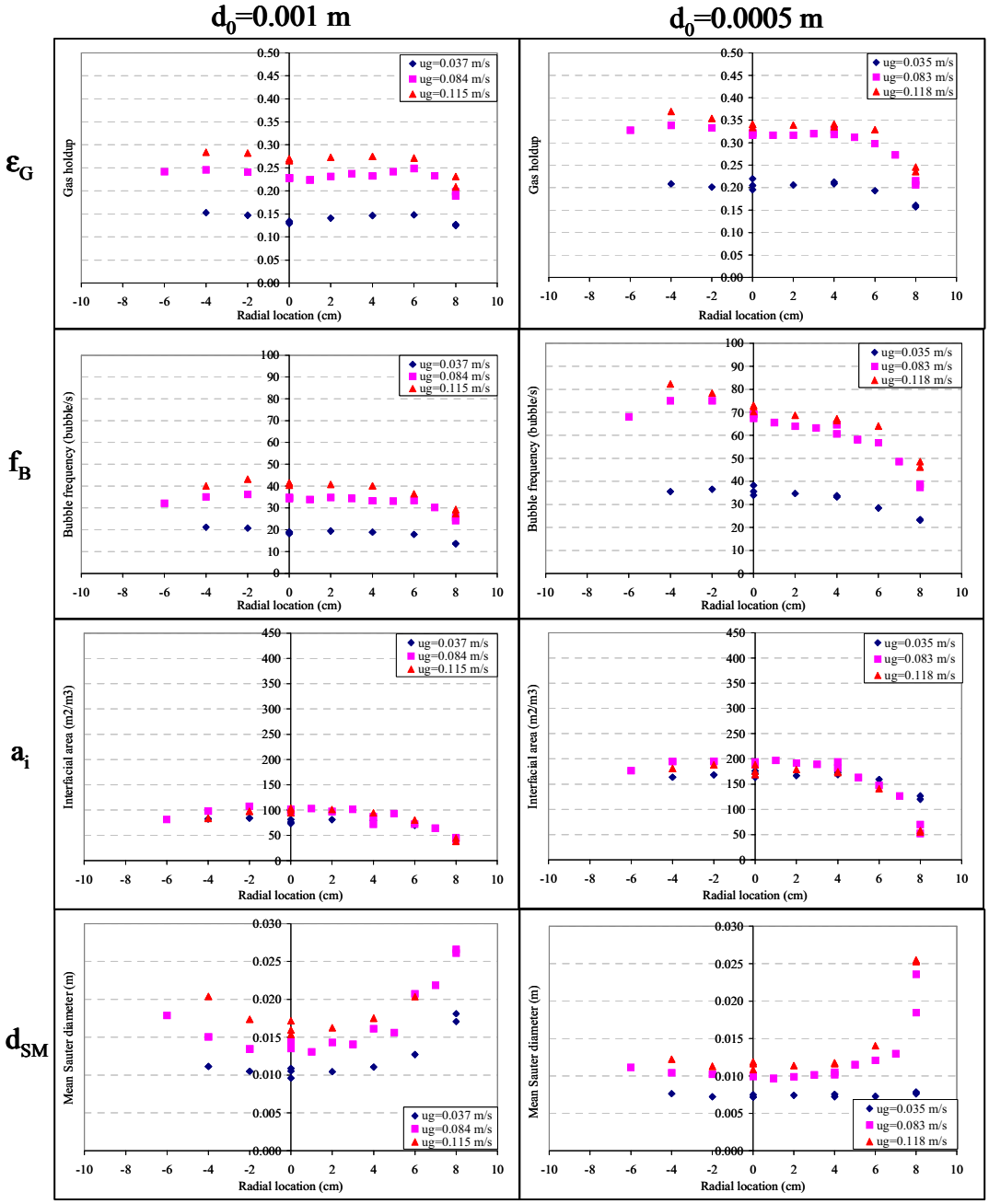


Figure 9. Local profiles at h=0.25 m

As for the interfacial area, it hardly depends on gas flow-rates and its values remain low (less than 100 $m^2/m^3$ for the large hole sparger and less than 200 $m^2/m^3$ for the small hole sparger).

## 3.4. Column bulk (h=0.65 m)

### 3.4.1. Radial profiles

Figure 10 presents the profiles observed in the column bulk (h=0.65 m) for each sparger.

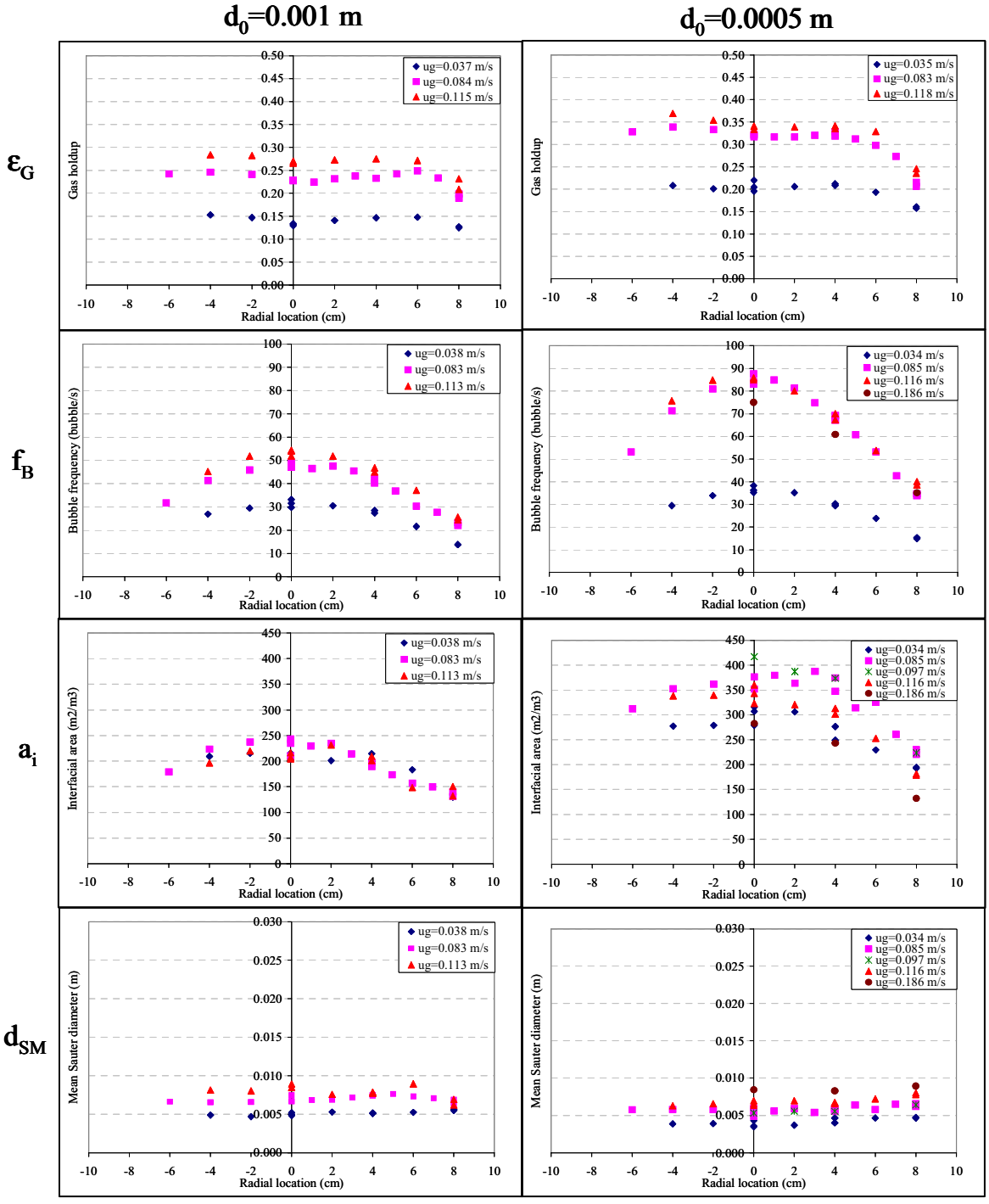


Figure 10. Local profiles at h=0.65 m for each sparger

#### 3.4.1.1. Bubbling regimes

When the bubbling regime is homogeneous, gas hold-up profiles are flatter than bubble frequency profiles. Concerning the bubble diameters, the profiles are flat; the mean bubble size stays between 0.003 and 0.005 m, depending on operating conditions.

At higher gas velocities, the gas hold-up and bubble frequency profiles are clearly higher and more parabolic than in the homogeneous regime. The mean bubble size also increases, but the profiles remain quite flat. Such a trend is difficult to comment on as the measured bubble size represents a mean value corresponding to upward bubbles and does not consider the whole bubble size distribution (Chaumat et al., in press). Concerning the interfacial area profiles, no clear gas velocity dependence can be observed due to the compensating effects of gas hold-up and bubble diameter.

When the heterogeneous regime is established ($u_G$>0.08 m/s), the profiles shape and values hardly evolve: the coalescence-break-up balance is established.

#### 3.4.1.2. Sparger effect

Radial profiles of gas hold-up and bubble frequency normalized by the value on the axis are compared on figure 11. The normalized gas hold-up shows that, in homogeneous and transition regimes, the profiles are more parabolic when increasing the gas velocity and using the large hole sparger. Conversely, the normalized bubble frequency profiles are surprising: the profile shapes are the same whatever the sparger and a priori whatever the superficial gas velocity and the hydrodynamics regime.

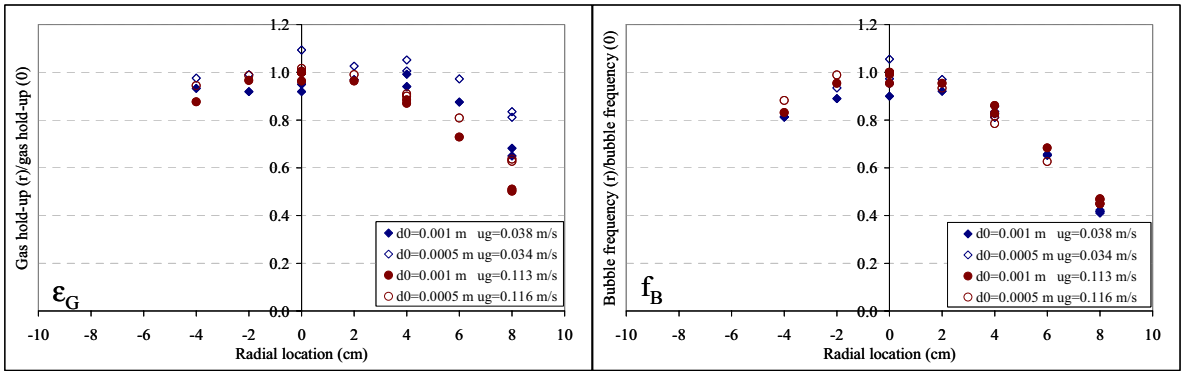


Figure 11. Normalized profiles in gas hold-up and bubble frequency at h=0.65 m

### 3.4.2. On column axis

Note that measurements realised on the column axis are more reliable than measurements realised near the wall because of the predominant ascendant mean flow direction (Chaumat et al., in press). To extend easily the investigated superficial gas velocity range and to draw clearer trends, more data has been performed on the column axis only. As the profiles shapes are all bell-shaped, those data can be compared.

#### 3.4.2.1. Gas hold-up

The gas hold-up axial data is plotted versus the gas velocity on figure 12. Its comparison with the mean gas hold-up in this area ($\varepsilon_{G,3}$) leads to profile shape deduction (fig. 12): the closer the global and local data are, the flatter the profile is. This comparison leads to observations similar to the previous measured profiles: the profiles shapes evolve gradually from flat profiles at low superficial gas velocity (in homogeneous regime) to parabolic profiles at higher gas hold-up. However, such a comparison gives shape profile estimation for a larger gas velocity range. Moreover, it could be used to determine more properly the regime transition: when the two gas hold-up curves deviate, the regime is not homogeneous yet. Note that, in this area, the bubbling regime transitions are located at the same gas velocities as in the whole column: a priori, the bubbling regimes do not depend on the position in the column.

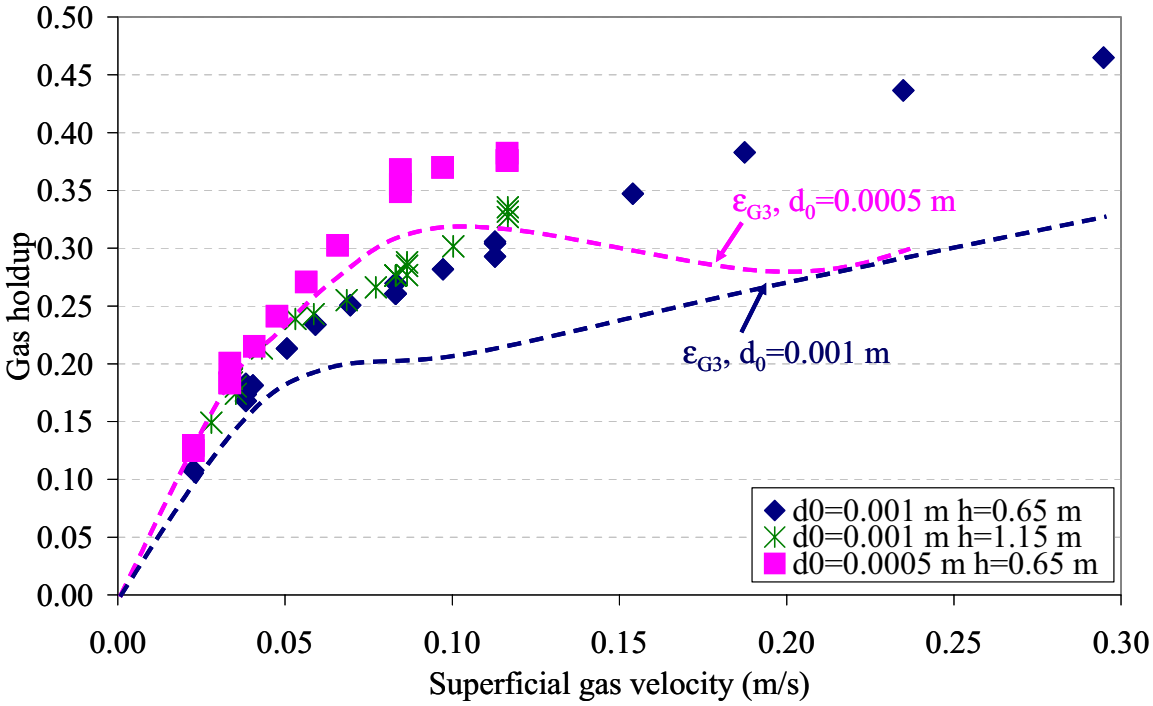


Figure 12. Comparison between local gas hold-up on the column axis and global gas hold-up

**3.4.2.2. Bubble velocity**

The same approach is applied to bubble velocity to estimate the profiles shapes: figure 13 presents simultaneously the local bubble velocity $v_B$ measured on the axis and the mean gas velocity $u_G/\varepsilon_{G,i}$ in the i section. Whatever the operating conditions, there is a wide difference between these two velocities which evidences large radial variations in bubble velocity whatever the superficial gas velocity. This confirms the observations of Yao et al. (1991) and Magaud et al. (2001): bubble velocity profiles can be parabolic even in the homogeneous regime.

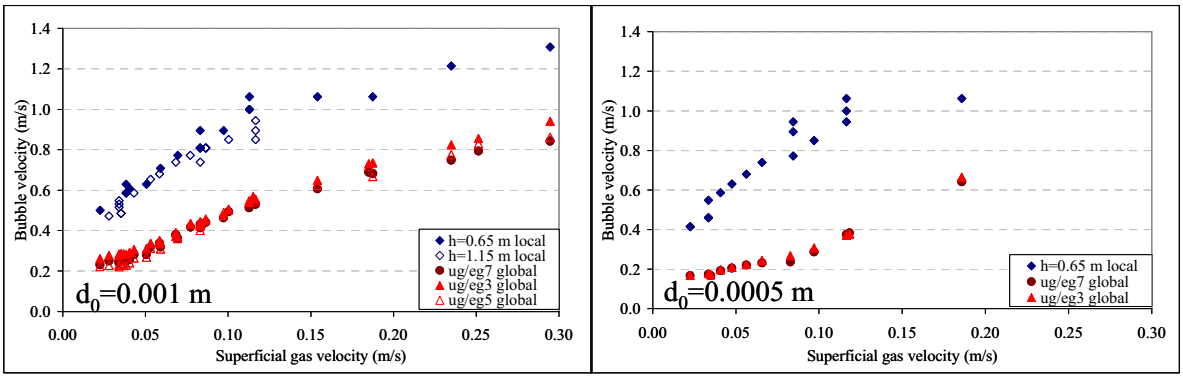


Figure 13. Comparison between gas phase velocity ($u_G/\varepsilon_{G,i}$) and bubble velocity ($v_B$) measured on the axis with the optic probe

**3.4.2.3. Interfacial area and bubble size**

At last, the central interfacial area and bubble size values are plotted for a large range of superficial gas velocity for each sparger (fig. 14).

In the homogeneous regime, the interfacial area clearly increases with regard to the superficial gas velocity, due to bubble number increase (gas hold-up and bubble frequency both increase). In this regime, the bubble diameter increases moderately (from 0.003 to 0.005 m approximately). Note that the homogeneous regime limit occurs for both spargers at the same bubble size (around 0.005 m).

In the transition regime, the interfacial area decreases (it is almost divided by two for the small hole sparger) due to bubble diameter increase (quite twofold): the coalescence phenomena are predominant.
Note that, in these two regimes, the bubble size is greater (and consequently the interfacial area smaller) with the large hole sparger. This could explain the homogeneous regime destabilization at a smaller gas velocity with this sparger, just as the smaller global gas hold-up.

In the heterogeneous regime, when the coalescence-break-up balance is established, the values of bubble size, interfacial area and gas hold-up on axis do not depend on the sparger. Moreover, the mean Sauter diameter does not evolve (the bubble diameter is about 0.009 m): the coalescence-break-up balance seems independent of gas velocity. The interfacial area increases again with regard to the gas flow-rate (the bubble number increase), but its evolution remains moderate; the interfacial area value is about 300 $m^2/m^3$ only.

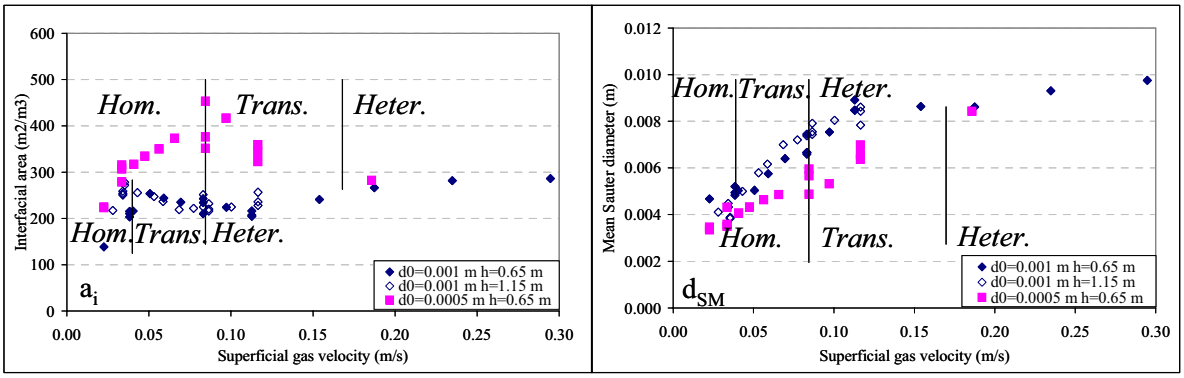


Figure 14. Interfacial area and mean Sauter diameter on axis for each sparger vs superficial gas velocity

## 3.5. Conclusion

This study in batch conditions is fruitful as it gives a complete flow description for a large range of gas velocities. Some specific radial and axial evolutions have then been brought to the fore.

On the other hand, it appears that the classical homogeneous regime description (no axial and radial flow evolution) is not realistic in these conditions, as it is too simplistic.
This analysis also shows that the normalized profiles of bubble frequency seem to be sparger and gas velocity independent.

# 4. EFFECT OF A LIQUID FLOW

## 4.1. Liquid flow characterization

In the case of continuous liquid flow, the liquid hydrodynamics can be described through RTD measurements. On figure 15, it appears that the equivalent CSTR number is only marginally altered by the sparger hole diameter ($d_0$=0.0005 or 0.001 m) and slightly diminishes when the superficial gas velocity increases (CSTR number diminution is comprised between 12 to 17% when $u_G$ increases from 0.04 to 0.13 m/s). The liquid velocity effect is more pronounced: the equivalent CSTR number clearly increases with the superficial liquid velocity (CSTR number increases about 25 to 35% when $u_L$ increases from 0.035 to 0.070 m/s). This significant superficial liquid velocity effect can be linked to a diminution of the liquid residence time in the column, whereas the superficial gas velocity effect is connected with more intense liquid loops, generated by central upflow and wall side downflow.

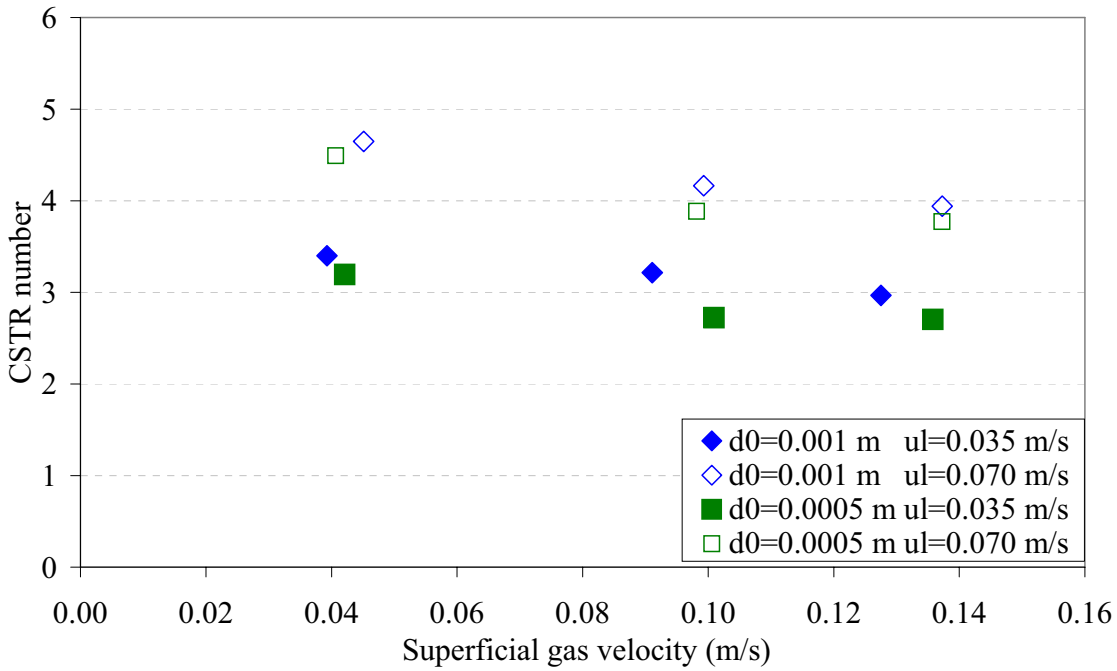


Figure 15. Global liquid hydrodynamics characterization through CSTR number

## 4.2. Global gas hold-up

Figure 16 shows that a continuous liquid flow modifies the mean gas hold-up values: the global gas hold-up systematically diminishes when the superficial liquid velocity increases, but the decrease extent depends on the operating conditions (superficial gas velocity and sparger).

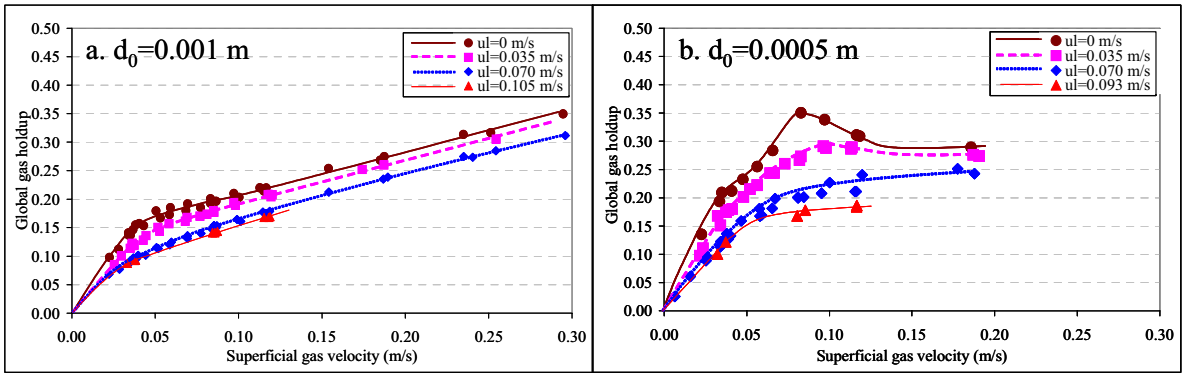


Figure 16. Liquid flow effect on global gas hold-up for each sparger

The hydrodynamics regime identification provides some explanations (fig. 17):

- When the heterogeneous regime is established whatever the liquid flow-rate ($u_G$>0.075 m/s for $d_0$=0.0001 m), the gas hold-up slightly decreases with the superficial liquid velocity due to an increase in the phase velocity $v_G$ by about $u_L/(1-\varepsilon_G)$: the bubbles are accelerated by the liquid stream.
- At smaller superficial gas velocity, the superficial liquid effect is more pronounced and more complex: the liquid circulation destabilizes the homogeneous flow, probably due to enhanced liquid turbulence and faster coalescence-break-up rates; it leads to the heterogeneous regime establishment at smaller superficial gas velocities. As a consequence, the sparger effect is reduced at high liquid velocity.

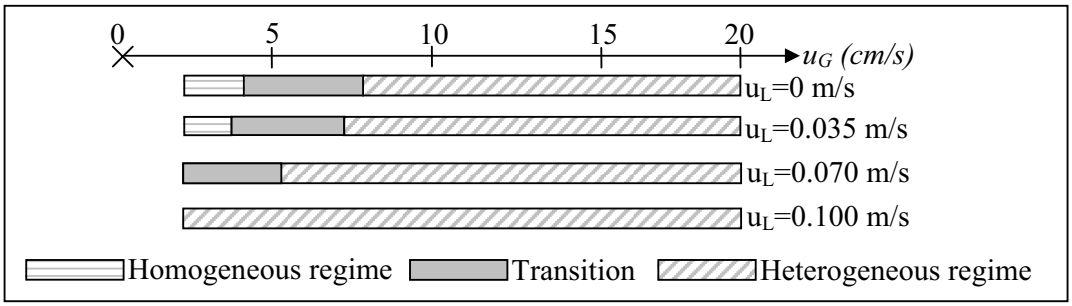


Figure 17. Bubbling regime identification with continuous liquid flow for $d_0$=0.001 m

### 4.3. Axial distribution of gas

In the column bulk, the gas hold-up axial evolution is similar with and without liquid flow (fig. 18). There is no clear axial evolution except at low gas velocity when the heterogeneous regime is not established yet.

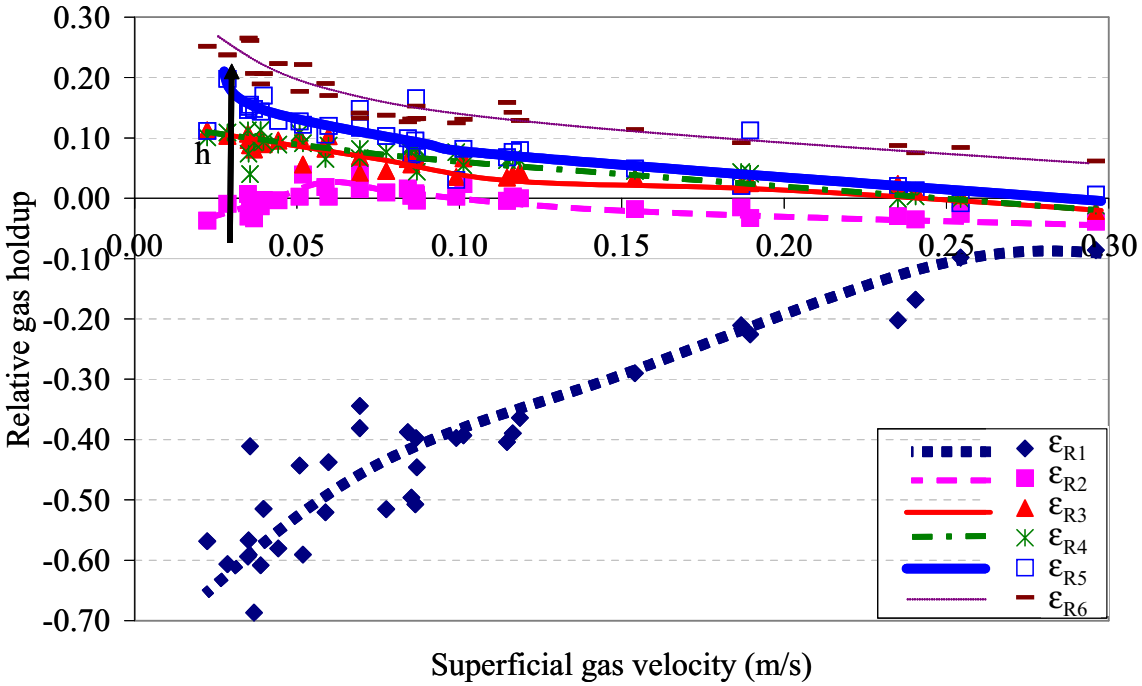


Figure 18. Axial evolution of the relative difference to the mean gas hold-up, obtained for $d_0$=0.001m sparger with $u_L$=0.070 m/s

However, the end areas differ clearly from batch case (fig. 18): the disengagement area is less pronounced than in batch conditions, whereas in the sparger area the mean gas hold-up $\varepsilon_{G,1}$ is always much lower than in the column bulk, unlike in batch conditions. The difference to the global gas hold-up varies in this area between 10 to 70% whereas it never exceeds 30% in batch liquid conditions. The liquid input probably hinders large liquid loops, which can not yet include the column bottom. Bubbles do not recirculate in the sparger area. Besides, the sparger area is higher than in batch conditions: it is not yet limited to the first 0.25 m (DP1 area), but includes partly the DP2 area, as $\varepsilon_{G,2}$ is slightly smaller than the bulk gas hold-up.
This analysis clearly shows that the superficial liquid velocity effect is very important, particularly at weak superficial gas velocity. It also stresses the need to analyze both the sparger and the bulk areas.

### 4.4. Column bottom analysis (h=0.25 m)

The liquid superficial gas velocity effect on the mean gas hold-up measured in the sparger area $\varepsilon_{G,1}$ is first evaluated (fig. 19). It appears that the liquid circulation effect is almost negligible for superficial liquid velocity less than 0.035 m/s (small decrease in gas hold-up) while the gas hold-up sharply diminishes when the superficial liquid velocity changes from 0.035 to 0.070 m/s: the mean gas hold-up is almost divided by two. This significant liquid effect is not extended by a further liquid velocity rise: the results obtained at $u_L$=0.105 m/s are similar to those obtained at $u_L$=0.070 m/s.

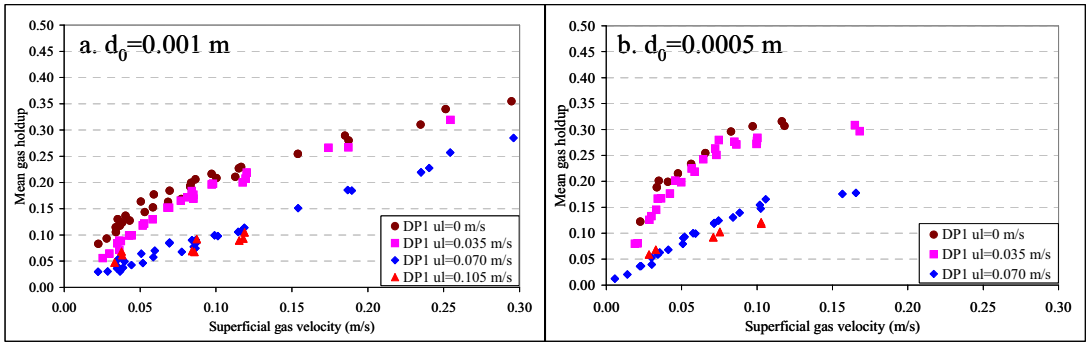


Figure 19. Liquid superficial velocity effect on the mean gas hold-up $\varepsilon_{G,1}$ (column bottom)

These trends on global data are verified on radial profiles (fig. 20): the profiles obtained at $u_L$=0 and 0.035 m/s are similar, and so are the profiles obtained at $u_L$=0.070 and 0.0105 m/s, but the profiles clearly differ between $u_L$=0.035 and 0.070 m/s: a more complex shape without modification of axis value is observed. As a conclusion, a minimum liquid velocity is needed to observe a clear influence but a further increase has no more effect. In our case this transition value of liquid velocity lies between 0.035 and 0.070 m/s.

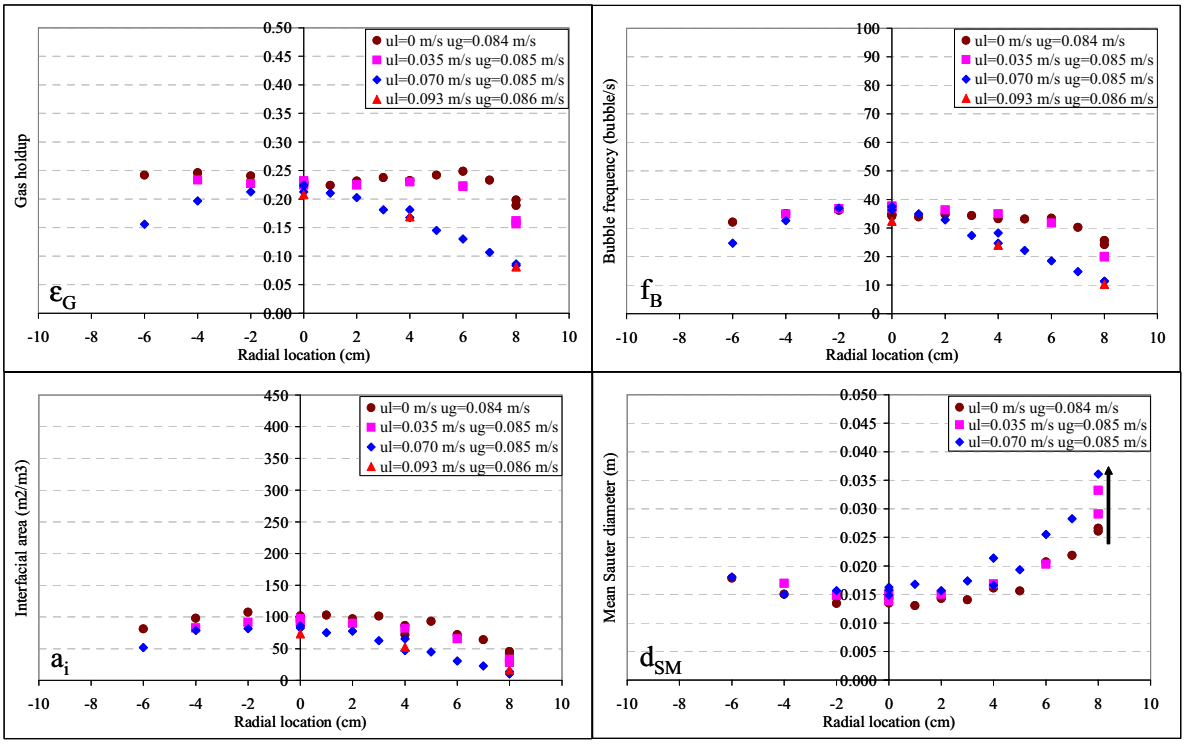


Figure 20. Local profiles at h=0.25 m for the large hole sparger ($d_0$=0.001 m)

Such a trend could be linked to the bottom geometry (fig. 21): at the bottom the liquid flow is restricted to a weak section near the wall, due to a redistribution plate and to the sparger rings. As this bottom geometry is specific to our pilot, this point is not detailed any more.

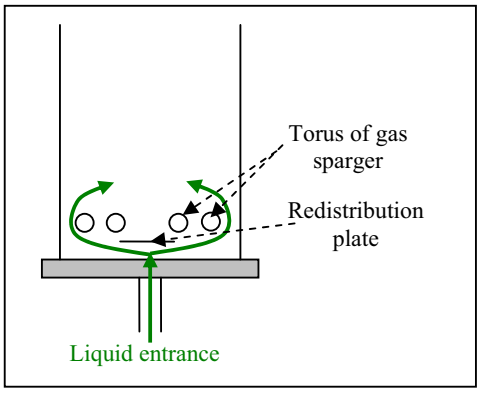


Figure 21. Gas and liquid injection area

## 4.5. Column bulk (h=0.65 m)

The mean gas hold-up in the column bulk $\varepsilon_{G,3}$ is not presented, because it is similar to the global data seen on figure 16.

### 4.5.1. Radial profiles

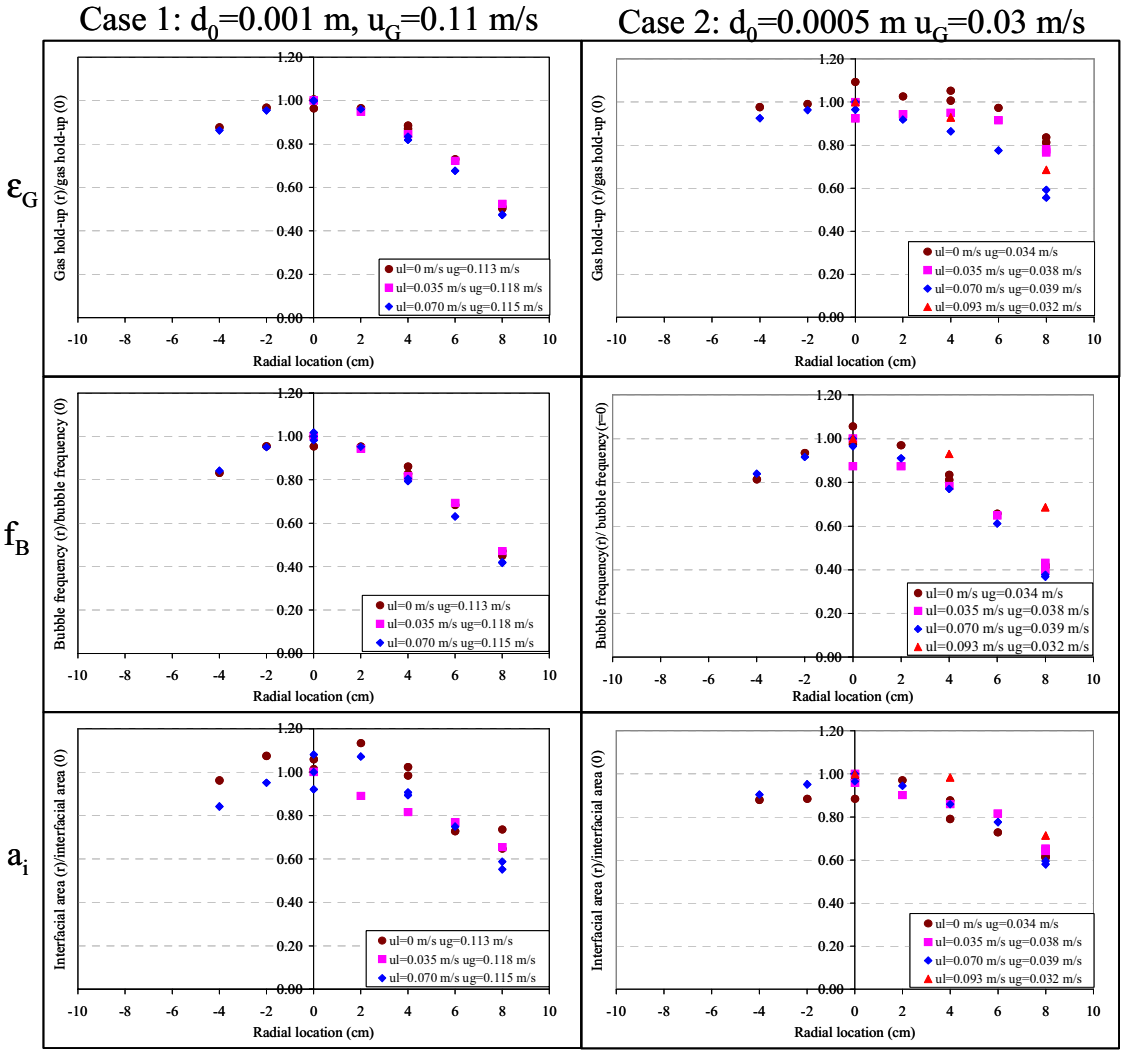


Figure 22. Superficial liquid velocity effect on the normalized profiles obtained at h=0.65 m in two operating conditions

The superficial liquid velocity effect is studied on profile shape (fig. 22). To make the comparison easier, figure 22 presents normalized profiles of gas hold-up, bubble frequency and interfacial area for two operating conditions: when the heterogeneous regime is established whatever the liquid velocity (case 1: $d_0$=0.001 m, $u_G$=0.11 m/s), and when there is a hydrodynamic regime change with $u_L$ (case 2: $d_0$=0.0005 m, $u_G$=0.03 m/s).

For case 1 ($d_0$=0.001 m, $u_G$=0.11 m/s), the liquid circulation does not affect the profile shapes of gas hold-up and bubble frequency. When the heterogeneous regime is established in batch, the liquid circulation effect is weak.

For case 2 ($d_0$=0.0005 m, $u_G$=0.03 m/s), the gas hold-up profile becomes more curved when the liquid velocity increases, according to the hydrodynamics regime change previously observed.

Note that, as in batch liquid conditions, the normalized frequency profiles are similar whatever the operating conditions.

**4.5.2. On column axis**

In order to determine the liquid and gas velocities effects on local data, the dimensional values are compared. As the profiles shapes do not deeply vary with regard to the operating conditions, only the axis values are plotted on figure 23.

Several observations are confirmed:

- At high superficial gas velocity, the superficial liquid velocity has few effects on the profiles: the flow structure is not modified. The liquid effect is limited to a bubble velocity increase which induces a diminution in bubble residence time, and therefore in mean gas hold-up.
- When the homogeneous or transition regimes are observed in batch range, the gas-hold-up, bubble frequency and interfacial area, diminish with $u_L$ and to a lesser extent the bubble diameter increases. That is in accordance with a transition to the heterogeneous regime.

As a conclusion, the liquid circulation effect can not be neglected at small gas hold-up, as it favors the heterogeneous regime transition. This effect is undesirable for mass transfer. At higher gas flow-rates, when the heterogeneous regime is established whatever the liquid velocity, the liquid circulation effect is softened; the liquid velocity influences only the gas and liquid residence time in the column.

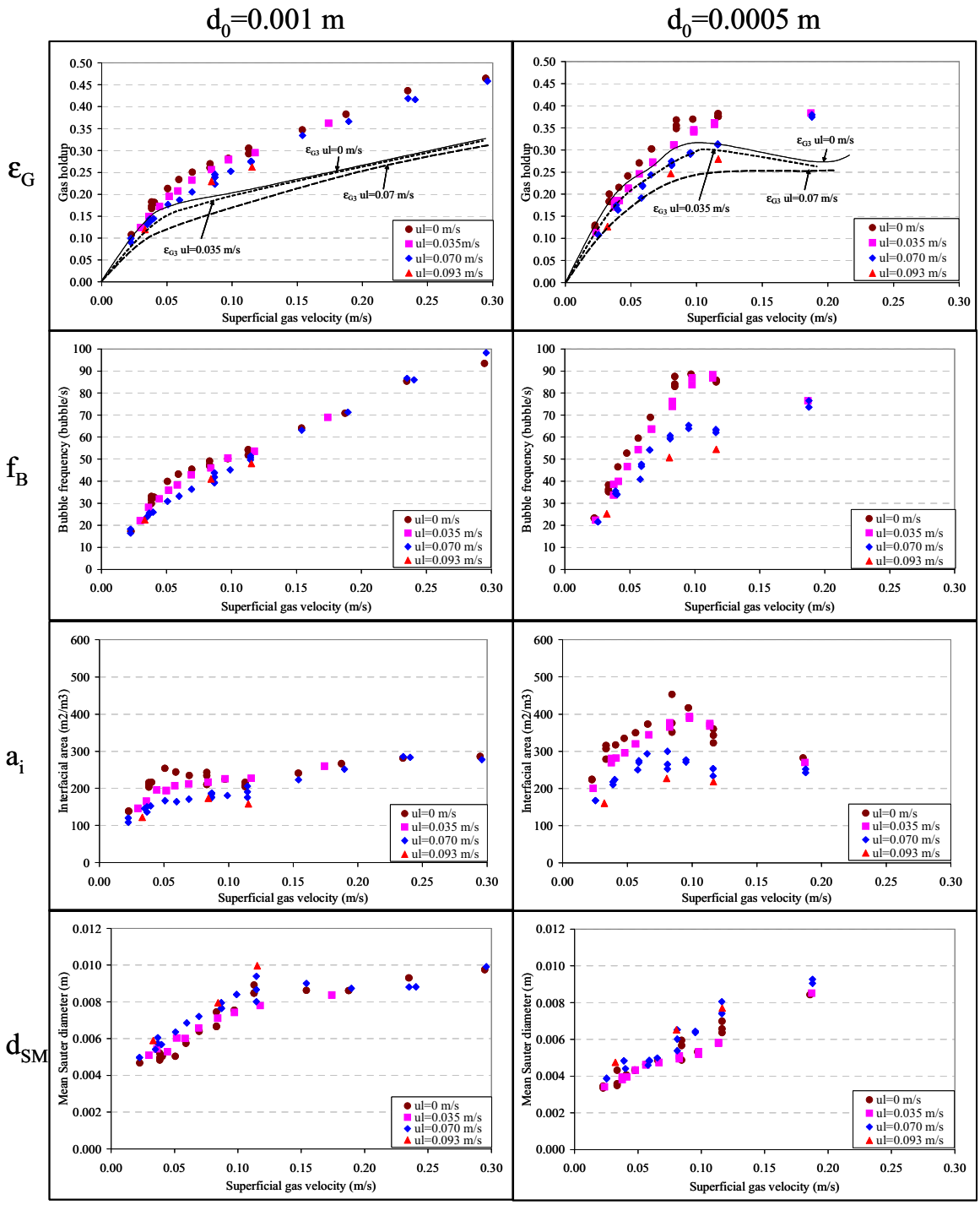


Figure 23. Superficial liquid effect on the axis values at h=0.65 m for each sparger

## 5. CONCLUSION

In this study, local data of gas hold-up, bubble frequency, bubble diameter and interfacial area, as well as global gas hold-up data, are measured at different axial and radial locations in a wide range of operating conditions. It leads to a rich database establishment and to a quite complete flow description. The local flow description shows that the local gas hold-up data are insufficient to describe the flow and that the knowledge of bubble frequency, bubble size and interfacial area brings some crucial complementary information. Among others, they bring to the

fore that, in any case in this work, bubbles near the sparger are always larger than in the higher column parts, even in the homogeneous regime; therefore the classical homogeneous regime description is then not adequate here.

The respective sparger, equilibrium and disengagement height have been evaluated. Each part's height depends on the sparger and on the superficial gas and liquid velocities.

In the column bulk, the mean gas hold-up continuously increases with axial position in the homogeneous and transition regime conditions (except at very low gas velocity, when the homogeneous regime is almost 'ideal'), whereas it is quite uniform in the heterogeneous regime. In this bulk area, the bubble diameter profiles are quite flat whatever the operating condition. The interfacial area slightly evolves at high gas velocity; it is about 300 $m^2/m^3$ on the column axis. It is also observed that the normalized bubble frequency profiles are the only normalized profiles which seem unchanged whatever the operating conditions.

The liquid circulation effect is the most interesting: an increase in the superficial liquid velocity induces a transition to the heterogeneous regime at moderate superficial gas velocity. In this case, the liquid velocity effect can not be neglected. At higher liquid and/or gas velocity, when the heterogeneous regime is established, a further increase in the liquid velocity only diminishes the residence time of the two phases.

This study with water allowed comparison with the prolific literature and a better knowledge of this pilot bubble flow. Such a study has also been performed in organic media (Chaumat, 2004), and will be published elsewhere.

## ACKNOWLEDGEMENTS

The financial support by Rhodia is acknowledged. We are grateful to Dr C. Mathieu and Dr F. Augier (Rhodia, Saint-Fons) for their help and constructive discussions.

## NOTATION

| | | |
|---|---|---|
| ai | Interfacial area | ($m^2/m^3$) |
| $d_0$ | Sparger orifice diameter | (m) |
| $d_P$ | Pore diameter of porous sparger | (m) |
| $d_{SM}$ | Mean Sauter diameter | (m) |
| $D_C$ | Column diameter | (m) |
| $DP_i$ | Differential pressure transducer i | |
| $f_B$ | Bubble frequency | (bubble/s) |
| g | Acceleration of gravity | ($m/s^2$) |
| h | Column axial location | (m) |
| $H_C$ | Column height | (m) |
| I | Ionic strength | (kg ion/$m^3$) |
| $l_{12}$ | Distance between optic probe tips | (m) |
| $N_{CSTR}$ | CSTR number | (-) |
| r | Radial location | (m) |
| $Re_0$ | Orifice Reynolds number | (-) |
| $u_G$ | Superficial gas velocity | (m/s) |
| $u_L$ | Superficial liquid velocity | (m/s) |

**Greek symbols:**

| | | |
|---|---|---|
| $\varepsilon_G$ | Gas hold-up | (-) |
| $\overline{\varepsilon}_G$ | Global mean gas hold-up | (-) |
| $\varepsilon_{G,i}$ | Mean gas hold-up on area i | (-) |
| $\mu_G$ | Gas viscosity | (Pa.s) |
| $\mu_L$ | Liquid viscosity | (Pa.s) |
| $\rho_G$ | Gas density | ($kg/m^3$) |
| $\rho_L$ | Liquid density | ($kg/m^3$) |
| $\sigma$ | Superficial tension | (N/m) |
| $\sigma^2$ | RTD variance | ($s^2$) |

| | | |
|---|---|---|
| $\tau$ | RTD mean residence time | (s) |

**Abbreviations:**

| | |
|---|---|
| CSTR | Continuous Stirred Tank Reactor |
| RTD | Residence Time Distribution |

## REFERENCES


Alvarez-Cuenca, M., Nerenberg, M.A, "Oxygen mass transfer in bubble columns working at large gas and liquid flow rates", AIChE J., Vol. 27, 66-73 (1981).

Anabtawi, M.Z.A., Abu-Eishah, S.I., Hilal, N., Nabhan, M.B.W., "Hydrodynamic studies in both bi-dimensional and three dimensional bubble columns with a single sparger", Chem. Eng. and Process., Vol. 42, 403-408 (2003).

Chaumat, H., "Hydrodynamique locale et globale d'une colonne à bulles en conditions industrielles", PhD thesis, INPT Toulouse, France (2004).

Chaumat, H., Billet-Duquenne, A.M., Augier, F., Mathieu, C., Delmas, H., "Mass transfer in bubble column for industrial applications. Effect of organic medium, gas and liquid flow rates and column design", Chem. Eng. Sci., Vol. 60, 5930-5936 (2005a).

Chaumat, H., Billet-Duquenne, A.M., Bascoul, A., Augier, F., Mathieu, C., Delmas, H., "Utilisation des capteurs de pression en colonnes à bulles industrielles : des mesures fiables et complètes", Récents Progrès en Génie des Procédés, Vol. 92, S-9, (2005b).

Chaumat, H., Billet-Duquenne, A.M., Augier, F., Mathieu, C., Delmas, H., "What is the reliability of an optical fiber probe when used in bubble column under industrial relevant conditions?", Exp. Thermal and Fluid Sci. (in press).

Chen, F., Gomez, C.O., Finch, J.A., "Technical note, Bubble size measurement in flotation machines", Minerals Eng., Vol. 14, 427-432 (2001).

Clark, N.N., Flemmer, R.L.C., "Turbulent circulation in Bubble Columns", AIChE J., Vol. 33, 515-518 (1987).

Degaleesan, S., Dudukovic, M., Pan, Y., "Experimental study of gas-induced liquid flow structures in bubble columns", AIChE J., Vol. 47, 1913-1931 (2001).

Dziallas, H., Michele, V., Hempel, D. C., "Measurement of local phase hold-ups in a Two-and Three-phase Bubble Column", Chem. Eng. Technol., Vol. 23, n°10, 877-884 (2000).

Fischer, J., Kamazawa, H., Sada, E., "On the local gas hold-up and flow pattern in standard-type bubble columns", Chem. Eng. and Process., Vol. 33, 7-21 (1994).

Groën, J.S., Müdde, R.F., van den Akker, H.E.A., "Time dependent behaviour of the flow in a bubble column", Trans. I. Chem. Engrs., Vol. 73, 615-621 (1995).

Hammer, H., Schrag, H., Hektor, K., Schonau, K., Kuster, W., Soemarno, A., Sakabi, U., Napp, W., "New sub-functions on hydrodynamics, heat and mass transfer for gas/liquid and gas/liquid/solid chemical and biochemical reactors", Front. Chem. Reac. Eng., 464 (1984).

Heijnen, J.J., Van't Riet, K., "Mass transfer, mixing and heat transfer phenomenon in low viscosity bubble column reactors", Chem. Eng. J., Vol. 28, B21-B52 (1984).

Joshi, J.B., Sharma, M.M., "A circulation cell model for bubble columns", Trans IChemE, Vol. 57, 244-251 (1979).

Kawase, Y., Umeno, S., Kimagai, T., "The prediction of gas hold-up in bubble reactors: Newtonian and non-newtonian fluids", The Chem. Eng. J., Vol. 50, 1-7 (1992).

Kemoun, A., Ong, B.C., Gupta, P., Al-Dahhan, M.H., Dudukovich, M.P., "Gas hold-up in bubble columns at elevated pressure via computed tomography", Int. J. of Multiphase Flow, Vol. 27, 929-946 (2001).

Luo, H., Svendsen, H.F., "Turbulent circulation in bubble columns from eddy viscosity distribution of single phase pipe flow", Can. J. Chem. Eng., Vol. 69, 1389-1394 (1991).

Magaud, F., Souhar, M., Wild, G., Boisson, N., "Experimental study of bubble column hydrodynamics", Chem. Eng. Sci., Vol. 56, 4597-4607 (2001).

Moustiri, S., Hébrard, G., Tharke, S.S., Roustan, M., "A unified correlation for predicting liquid axial dispersion coefficient in bubble columns", Chem. Eng. Sci., Vol. 56, 1041-1047 (2001).

Parasu Veera, U., Kataria, K.L., Joshi, J.B., "Gas hold-up profiles in foaming liquids in bubble columns", Chem. Eng. J., Vol. 84, 247-256 (2001).

Reilly, I.G., Scott, D.S., de Bruijn, T.J.W., Jain, A.K., Piskorz, J., "A correlation for gas hold-up in turbulent bubble column", Can. J. of Chem. Eng., Vol. 64, 705-717 (1986).

Shah, Y.T., Kelkar, B.G., Godbole, S.P., Deckwer, W.-D., "Design parameters estimations for bubble column reactors", AIChE J., Vol. 28, n°3, 353-378 (1982).

Sotelo, J.L., Benitez, F.J., Beltran-Heredia, J., Rodriguez, C., "Gas hold-up and mass transfer coefficients in bubble column. 1. Porous glass-plate diffusers", Int. Chem. Eng., Vol. 34, n°1, 82-90 (1994).

Yang, G.Q., Fan, L.S., "Axial liquid mixing in high-pressure bubble columns", AIChE J., Vol. 49, 1995-2008 (2003).

Yao, B.P., Zheng, C., Gasche, H.E., Hofman, H., "Bubble behaviour and flow structure of bubble columns", Chem. Eng. Process, Vol. 29, 65-75 (1991).

Zheng, C., Yao, B., Feng, Y., "Flow Regime Identification Gas Hold-up of Three-phase Fluidized Systems", Chem. Eng. Sci., Vol. 43, n°8, 2195-2200 (1988).